



The Remarkable Outer Hair Cell: Proceedings of a Symposium in Honour of W. E. Brownell

Jonathan F. Ashmore¹ · John S. Oghalai² · James B. Dewey² · Elizabeth S. Olson³ · Clark E. Strimbu³ · Yi Wang³ · Christopher A. Shera⁴ · Alessandro Altoè⁴ · Carolina Abdala⁵ · Ana B. Elgoyhen⁶ · Ruth Anne Eatock⁷ · Robert M. Raphael⁸

Received: 22 December 2021 / Accepted: 2 May 2022

© The Author(s) under exclusive licence to Association for Research in Otolaryngology 2023

Abstract

In 1985, Bill Brownell and colleagues published the remarkable observation that cochlear outer hair cells (OHCs) express voltage-driven mechanical motion: electromotility. They proposed OHC electromotility as the mechanism for the elusive “cochlear amplifier” required to explain the sensitivity of mammalian hearing. The finding and hypothesis stimulated an explosion of experiments that have transformed our understanding of cochlear mechanics and physiology, the evolution of hair cell structure and function, and audiology. Here, we bring together examples of current research that illustrate the continuing impact of the discovery of OHC electromotility.

Keywords Electromotility · Prestin · Cochlear amplifier · Optical coherence tomography · Otoacoustic emissions · Efferent

Introduction

In 1985, Brownell, Bader, Bertrand, and de Ribaupierre reported that outer hair cells (OHCs), which are unique to mammalian cochleas, express significant voltage-driven

motion, or *electromotility*. They proposed that OHC electromotility could represent the cochlear amplifier originally proposed by Thomas Gold (Gold 1948) to account for the wide dynamic range of hearing. Bill Brownell introduced these findings and ideas to an amazed assembly of hearing researchers attending the 1984 Midwinter Meeting of the Association for Research in Otolaryngology (ARO). The impact on our understanding of hearing was both immediate and long-lasting, galvanizing researchers in areas ranging from inner ear biophysics to clinical testing for hearing impairment and attracting new investigators from outside hearing research. Despite tremendous progress in the last 35 years, many questions remain about the mechanism and function of outer hair cell electromotility—including how it evolved, how it can operate at high frequencies, how it contributes to overall cochlear mechanics, and how it relates to otoacoustic emissions (sounds produced by the cochlea that can be recorded with a microphone in the ear canal).

To celebrate Bill’s achievement and highlight how it continues to drive research, the ARO held a symposium at the 44th Midwinter Meeting in 2021: “The Remarkable Outer Hair Cell: Symposium in Honor of Bill Brownell.” This report brings together contributions from the speakers and their collaborators. Jonathan Ashmore discusses how OHCs transduce voltage into the mechanical energy of motility. John Oghalai and Elizabeth Olson and colleagues show how

✉ Robert M. Raphael
rraphael@rice.edu

¹ UCL Ear Institute, University College London, London, UK

² Department of Otolaryngology-Head and Neck Surgery, University of Southern California, Los Angeles, USA

³ Department of Otolaryngology Head and Neck Surgery, Vagelos College of Physicians and Surgeons, Columbia University, New York City, USA

⁴ Caruso Department of Otolaryngology and Department of Physics and Astronomy, University of Southern California, Los Angeles, USA

⁵ Caruso Department of Otolaryngology, University of Southern California, Los Angeles, USA

⁶ Instituto de Investigaciones en Ingeniería Genética y Biología Molecular “Dr. Héctor N. Torres” (INGEBI), Consejo Nacional de Investigaciones Científicas y Técnicas (CONICET), Buenos Aires, Argentina

⁷ Department of Neurobiology, University of Chicago, Chicago, USA

⁸ Department of Bioengineering, Rice University, Houston, USA

visualizing sound-evoked motions of structures inside the cochlea reveals interactions between OHC electromotility and other features to produce amplification. Christopher Shera and Alessandro Altoè show that tapering of cochlear structures with position, rather than tonotopy of OHC properties, produces tonotopic variation in sound-evoked responses. Carolina Abdala describes new approaches to measuring and analyzing otoacoustic emissions as an accessible indicator of cochlear dysfunction. Ana Belén Elgoyhen shows how the cholinergic receptor proteins that mediate efferent feedback on vertebrate hair cells have undergone selective evolutionary pressure in OHCs.

Molecular and Cellular Mechanisms of Outer Hair Cell Electromotility

Jonathan F. Ashmore

Following the discovery that outer hair cells undergo mechanical deformation in response to electrical stimulation, the goal of understanding the molecular and cellular basis of electromotility has been a “Holy Grail” of auditory biophysics. Jonathan Ashmore describes recent developments in this quest to understand the structural basis of outer hair cell function.

It is hard to realize that only a few decades ago, the mechanistic role of outer hair cells (OHCs) in cochlear amplification was far from clear although it was appreciated that OHCs were involved in an essential way. The 1985 paper opened up a whole new era of thinking about OHCs: it showed that single cells were electro-motile, lengthening when hyperpolarized and shortening when depolarized (Brownell et al. 1985). The mechanism turned out to be fast enough to be involved in cochlear mechanical tuning and to underpin the requirement of a cochlear amplifier, a mechanism hinted at in earlier hypotheses of how to cancel the viscous damping in the cochlear partition (Gold 1948).

The molecular basis for electromotility is the protein prestin. It was identified in 2000 by the Dallos laboratory from a subtracted hair cell DNA library (Zheng et al. 2000). The

surprise is that prestin is not a conventional motor molecule: it is a member of the SLC26 family of membrane transporters, probably forming a tetrameric assembly in the lateral membrane of the OHC. Prestin (SLC26A5) can act as a low-efficiency chloride-bicarbonate counter-transporter (Mistrik et al. 2012) and so regulate the intracellular pH of the OHCs. In OHCs, its function is largely dominated by an incomplete transport cycle, where the chloride ion is moved from the cytoplasm into the membrane field in the inward-facing vestibule of the tetramer (Fig. 1). This could produce conformational change without moving chloride across the membrane.

The idea that co-transporter mechanisms have been co-opted for electromotility has remained speculative but has received support from recent structural determinations of mammalian prestin/SLC26A5 (Bavi et al. 2021; Butan et al. 2022; Ge et al. 2021). First steps in this direction came from published structures of the bacterial ortholog, DgSLC26, which was found to be an obligate dimer (Geertsma et al. 2015). A closely related member of the same protein family, SLC26A9, is also a dimer with an unusual oligomerization interface in the cytoplasmic portion of the molecule between the STAS domains (Walter et al. 2019). These data suggest that prestin/SLC26A5 has a particular conformation in situ which could be tetrameric, as many lines of evidence have indicated.

A cochlear amplifier based on simple OHC electromotility faces a problem: it is a mechanism driven by transmembrane potential. The filtering by the membrane time constant may limit bandwidth for electromotility although it can be argued that the electrical time constant is substantially reduced towards the cochlear base (Johnson et al. 2011). An idea which now seems plausible is that power can still be delivered to the mechanics if the prestin-based mechanism is modelled as a piezo-electric actuator (Iwasa 2017; Rabbitt 2020). This has been addressed by data recorded from macropatches of the OHC membrane (Santos-Sacchi & Tan 2020). In the case which applies to an OHC mechanically constrained in the intact cochlea, the anion movements through prestin generate sufficient current to cancel the capacitance effects of the membrane. Such a possibility

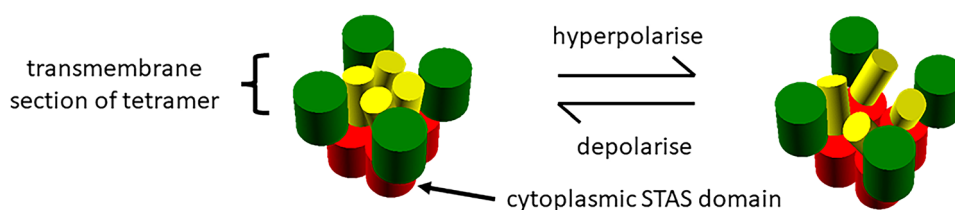


Fig. 1 A scheme for prestin/SLC26A5 function in the OHC membrane. The 8-nm particle seen by electron microscopy is a tetramer, a dimer of dimers, formed from the basic 8kDa molecule. Each of the molecule's 14 transmembrane regions is embedded in the membrane

and the STAS domain is in the cytoplasm. Hyperpolarization results in anions moving in the cytoplasmic vestibule and producing up to 4% increase in particle diameter in the plane of the membrane. High molecular crowding then results in the OHC elongating

extends the frequencies over which the OHC population can determine the mechanics of the cochlea.

Non-invasive Studies of Cochlear Amplification In Vivo

James B. Dewey and John S. Oghalai

Ex vivo experiments on OHCs present unsolved problems for a variety of technical reasons, including the inaccessibility of the basal cochlea, the limited bandwidth of patch clamp techniques and the relative experimental fragility of the cells. The emerging complementary approach of optical coherence tomography (OCT) overcomes these problems, as discussed in the next two segments by John Oghalai, Elizabeth Olson and their collaborators.

Ever since the discovery that the OHCs change length in response to electrical stimulation (Brownell et al. 1985), experimentalists and modellers have sought to understand how this electromotility might be responsible for amplifying sound-evoked vibrations within the cochlea—a process that is essential for mammalian hearing sensitivity (Ashmore 2008; Dallos et al. 2006; Fettiplace 2020). The dominant view is that OHC electromotility delivers force to the underlying basilar membrane (BM) on a cycle-by-cycle basis, thus enhancing the cochlear travelling wave as it propagates from base to apex (de Boer 1983; Neely and Kim 1983). However, for this scheme to work across the frequency range of mammalian hearing, which can extend beyond 100 kHz (Vater and Kössl 2011), OHC electromotility must be capable of operating at remarkable speeds.

Two key issues have led to ongoing debate regarding the ability of OHC electromotility to subserve high-frequency amplification. The first is whether electromotility can faithfully follow rapid changes in voltage. While the pioneering

study of Frank et al. (1999) demonstrated that electrically stimulated and mechanically constrained OHCs can generate nearly constant force up to at least 50 kHz, recent measurements have characterized electromotility as inherently low-pass in nature (Santos-Sacchi et al. 2019; Santos-Sacchi and Tan 2018). The second issue is the OHC membrane's electrical impedance, which low-pass filters the transmembrane potential that drives electromotility (Housley and Ashmore 1992; Johnson et al. 2011; Mammano and Ashmore 1996). Given these limitations, it is unclear if meaningful cycle-by-cycle length changes are even elicited by high-frequency sound in vivo.

We recently examined the efficacy of high-frequency OHC electromotility in vivo by using an optical coherence tomography (OCT)-based approach to noninvasively image through the cochlear bone in live adult mice (Fig. 2a) and measure sound-evoked displacements from within the organ of Corti (Dewey et al. 2021). The relevant methodology has been detailed previously (Dewey et al. 2019; Gao et al. 2014; Lee et al. 2015). Through careful spatial mapping of the vibratory responses, we showed that high-frequency sounds cause the top and bottom of the OHC region to move in opposite directions, both tonically and on a cycle-by-cycle basis (Fig. 2b–c). These motions resemble OHC length changes observed in vitro (Ashmore 1987; Brownell et al. 1985) and are consistent with the OHC's electromotile response to tonic and cycle-by-cycle changes in its transmembrane potential. By studying displacement responses at the stimulus frequency and its harmonics, we found that the out-of-phase motions occur at frequencies more than twice the local characteristic frequency. While we saw evidence of low-pass filtering in the displacements, similar to what has been shown in gerbil (Vavakou et al. 2019), motions within the OHC region were still larger than the motion of the underlying BM at all frequencies. These measurements indicate that substantial OHC electromotility is elicited by

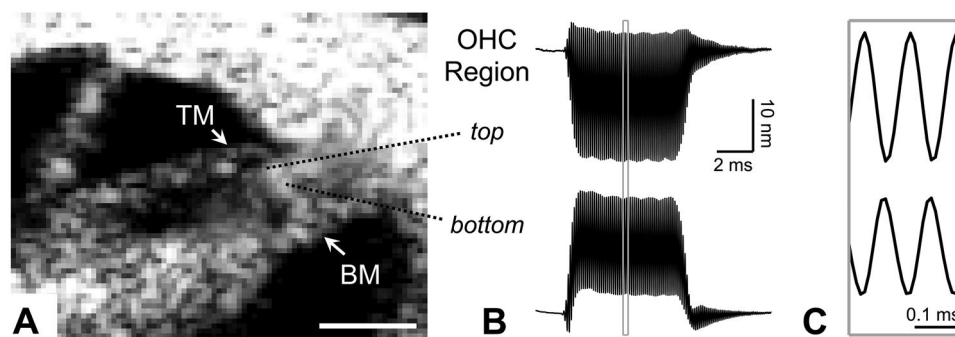


Fig. 2 OCT shows cycle-by-cycle OHC electromotility evoked in vivo by high-frequency tone bursts. **A** OCT image of the apical turn of the mouse cochlea. TM tectorial membrane. Scale bar=100 μ m. **B** Displacement waveforms of the top and bottom of the OHC region elicited by a 60-dB SPL tone presented at 9 kHz. The asymmetry in the

responses reveals a tonic shift in the position of the top and bottom of the OHC region toward one another during the stimulus. **C** High-lighted portion of response in **B** on a shorter time scale, showing that the top and bottom of the OHC region move out of phase with each stimulus cycle

high-frequency sound *in vivo*, and support the notion that electromotility underlies mammalian cochlear amplification.

Probing the Relationship Between OHC Electromotility and Cochlear Amplification

Elizabeth S. Olson, C. Elliott Strimbu and Yi Wang

The fundamental signature of the cochlear amplifier is the active, nonlinear tuning of the basilar membrane (BM) at frequencies close to a given location's best frequency (BF). This aspect of the cochlear amplifier was discovered by Rhode (Rhode 1971). Other discoveries supporting the idea that the cochlea was active soon followed: acoustic emissions (Kemp 1978), electrically-induced changes in cochlear mechanics (Hubbard and Mountain 1983), mechanical tuning that was as sharply tuned as auditory nerve fibres (Khanna and Leonard 1982), and nonlinear models of cochlear activity (Kim et al. 1973). It was into this fertile territory

that the discovery of outer hair cell (OHC) electromotility arrived (Brownell et al. 1985) and the OHC was adopted as the putative active element driving cochlear amplification.

In mammalian cochleas, the endolymph bathing the mechanosensitive hair bundles has a high positive potential (+80 to 90 mV) which increases the driving force for current through transduction channels and affects the voltage across the prestin-containing basolateral membrane of OHCs. This endocochlear potential (EP) can be reduced or eliminated by intravenous (IV) furosemide. Olson and colleagues used this tool to manipulate EP and observe the impact on cochlear mechanics (Strimbu et al. 2020; Wang et al. 2019). These measurements used an OCT system (Thorlabs), a relatively new technology that allows for imaging and vibrometry within the sensory tissue (Olson and Strimbu 2020; Strimbu et al. 2020). The results show that there is more to cochlear amplification than OHC electromotility.

Figure 3 a shows the progression of displacement responses of the basilar membrane (BM) and OHC regions,

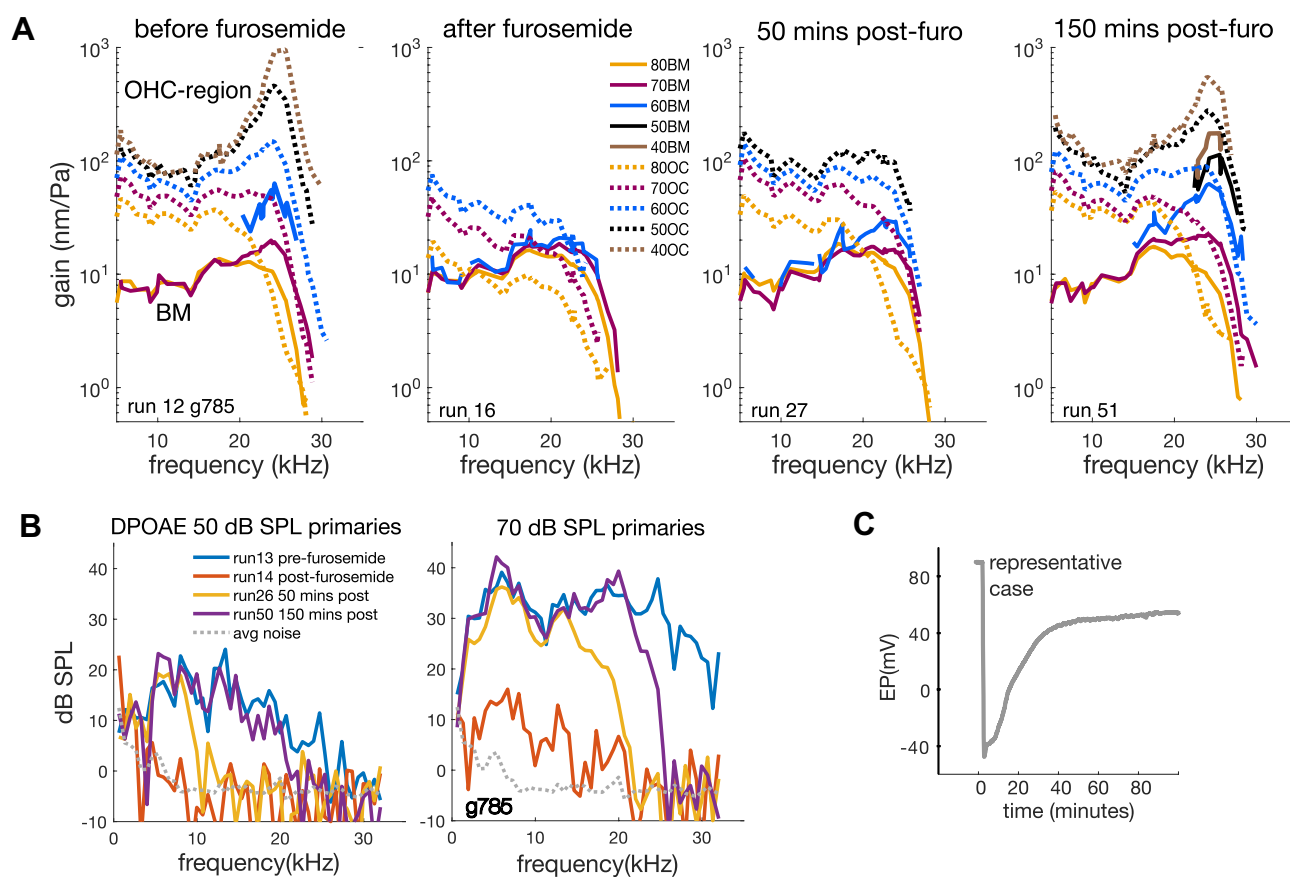


Fig. 3 Furosemide effects on simultaneous sound-evoked displacements at two locations, the BM and OHC regions, distinguish components of the cochlear amplifier. **A** Amplitude is shown as gain by normalizing to sound pressure level (SPL). Only amplitude is shown; furosemide-induced changes to phase were minimal. The multi-tone sound stimulus was presented closed-field at the SPLs indicated in the

legend (range 40–80 dB SPL). Measurements are shown before IV furosemide injection and several minutes, 50 min and 150 min after. **B** DPOAE measured at approximately the same time points as in **A**, in the same preparation. **C** Representative EP measurement following IV furosemide, from a different preparation. The effect of IV furosemide on EP was consistent across preparations (Wang et al. 2019)

with time following furosemide injection. Before furosemide injection, the BM region (solid curves) was tuned and nonlinear in the best frequency (BF, ~23 kHz) band (see increasing gain as stimulus level decreased from 80 to 60 dB SPL). In the sub-BF band (below 20 kHz), the BM region responded linearly to changes in level. In contrast, OHC responses (dashed curves) were larger and nonlinear in the sub-BF band. Sub-BF nonlinearity was also present in OHC electrical responses measured close to the sensory tissue. The sub-BF nonlinearity in OHC region motion likely reflects the nonlinearity of OHC electromotile responses, in turn reflecting the nonlinear scaling of the OHC current that drives electromotility (Fallah et al. 2019).

Following furosemide, the BM region motion response was reduced and became approximately linear, such that gain-frequency plots were similar for different input levels at all frequencies, including at and above BF. In contrast, the OHC response was reduced and lost the BF peak but retained nonlinearity at all frequencies.

Figure 3 c shows, in a different, representative animal, the time course of the effect of furosemide IV injection on EP. By 40–50 min, EP had substantially, but not completely, recovered and stabilized. Similarly, sub-BF nonlinearity in OHC motion had fully recovered (see 50-min data in Fig. 3a). However, the tuned, nonlinear BF peak of OHC motion was still diminished; its recovery mainly occurred between 50 and 150 min, a time window corresponding to stable, sub-normal EP (Fig. 3c). OHC electromechanical activity is also reflected in measurements of distortion product oto-acoustic emissions (DPOAEs), further described below. DPOAEs at the BF of the motion measurements (~24 kHz) also recovered between 50 and 150 min (Fig. 3b).

Thus, while OHC electromotility and EP recover on similar timescales, other elements of cochlear mechanics that are perturbed by the low EP take longer to recover. One interpretation of these observations is that the recovery of these (still mysterious) elements allows OHC electromotility to successfully engage within the mechanics of the cochlea, to produce the greatly enhanced motion and frequency selectivity that is required for normal hearing. Perturbation studies such as this allow us to probe the constellation of factors that together produce healthy cochlear amplification.

Hair Cells or Geometry? Accounting for Tonotopic Variations in Cochlear Response Properties

Christopher A. Shera and Alessandro Altoè

The discovery of OHC electromotility followed closely after the discovery by Kemp (1978) that the inner ear produces sounds, which are now called otoacoustic emissions (OAEs). OAEs were quickly recognized as providing strong evidence for cochlear amplification, in addi-

tion to being valuable noninvasive indicators of cochlear health. The relation between OAEs, cochlear mechanics, and outer hair cell activity is an area of intense research. Below, Shera and Altoè reinforce that passive, geometric properties of the cochlea are the substrate for cochlear tuning on which OHCs operate. They analyze how the tapered shape of the cochlea affects spatial variations in cochlear gain, frequency tuning, and response delays.

The physical structure of the cochlea gives it remarkable acoustic properties. When queried with a click, the cochlea responds with a brief “sound rainbow,” a chirp-like echo in which different frequencies return at different times (Kemp 1978). The echoed sounds, known as click-evoked otoacoustic emissions, arise when pressure waves travelling along the cochlear spiral encounter mechanical irregularities in the organ of Corti and scatter back coherently (Zweig and Shera 1995). The sound rainbow reveals important information about how the inner ear processes and analyzes sound. At the broadest level, of course, it shows that the cochlea processes different sounds differently. More particularly, because the cochlea maps frequency onto position, the variation of frequency with time can be reinterpreted as the variation of response delay with cochlear location. That delay, in turn, reveals details of cochlear frequency analysis (Shera et al. 2010). As a well-known example, the rainbow confirms that the sharpness of cochlear tuning varies systematically, being considerably sharper in the cochlear base than in the apex. How do these spatial variations in cochlear signal processing arise?

Biases in our thinking encourage us to seek explanations for the behaviour of complex systems in the properties of their components. And what, fundamentally, is the cochlea but an array of hair cells tuned to different frequencies? It is therefore no great leap to hypothesize that the answer lies there, somewhere in the hair cells. Indeed, many characteristics of hair cells are known to vary along the length of the cochlea, including their sizes and orientation within the organ of Corti, the conductances of their mechano-electric transduction channels, and the rate constants of their adaptation kinetics (e.g., Johnson et al. 2011). Nevertheless, we set out to test the hypothesis by assuming the contrary (Altoè and Shera 2020a). For purposes of argument, we therefore assume that outer hair cells—aside from whatever contributions they make to determining the local characteristic frequency (CF) (Tobin et al. 2019)—are otherwise functionally identical.¹ We implement this assumption in a cochlear model (3D, inviscid fluid) by assuming that the active admittance characterizing the bulk motion of the organ of Corti (adapted from Altoè and Shera 2020b) is scaling symmetric.

¹ One could say that we take seriously the title of this symposium: “The Remarkable Outer Hair Cell,” with an emphasis on the *The*, as if there were only one. Not literally *one*, of course, as Wheeler and Feynman proposed for the electron, but rather a uniform array with no particular spatial gradient in biophysical response properties other than those arising from—or contributing to—the cochlear map.

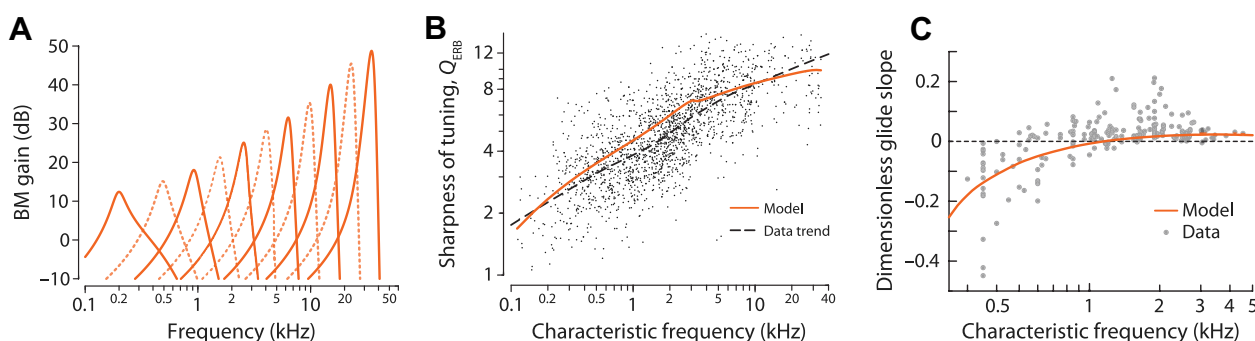


Fig. 4 Model results demonstrate that cochlear geometry can account for observed spatial variations in three measures of cochlear signal processing in cat. **A** Basilar-membrane (BM) transfer functions (BM velocity re: pressure at the stapes) computed at 11 locations. **B** Variation in the sharpness of mechanical frequency tuning (quantified as Q_{ERB}) compared with values obtained from the cat auditory nerve

(Cedolin and Delgutte 2005). **C** Variation and sign reversal in the dimensionless glide slope (defined at the time rate of change of the instantaneous frequency of the BM click response, normalized by the square of the local CF) compared with values from the cat auditory nerve (Carney et al. 1999; Shera 2001).

Adapted from Fig. 3 of Altoè and Shera (2020a)

In other words, we assume there are no gradients in cochlear micromechanics other than those contributing to the tonotopic map. If the OHCs in the model do not vary, what does? In a nutshell, we include known macromechanical gradients in cochlear geometry while keeping micromechanical tuning the same at all locations. Thus, we incorporate the cochlear tonotopic map, including its nonexponential form in the apex, and the well-known gradient in basilar-membrane stiffness. And, very importantly, we also incorporate realistic tapering of the cross-sectional area of the cochlear duct.

Remarkably, this simple model accounts for a number of prominent apical-basal differences (Altoè and Shera 2020a).

Figure 4 demonstrates that the model's responses (shown in orange) nicely reproduce the physiological trends, including apical-basal changes in the shapes of transfer functions (Fig. 4A), the sharpness of tuning (Fig. 4B), and the “glide” in the instantaneous frequency of the response to acoustic clicks (Fig. 4C). Thus, global variations in cochlear geometry appear sufficient to account for the data. Evidently, our initial hypothesis was incorrect: spatial gradients in cochlear micromechanics or OHC properties are not needed. Aside from their CF, the outer hair cells, remarkable as they are, might as well all be identical. How does cochlear geometry produce these spatial variations? Although there are multiple factors involved, arguably, the most important contribution comes from the tapering of the cochlear duct (see also (Puria and Allen 1991; Sasmal and Grosh 2019; Shera and Zweig 1991)). To appreciate the effects of tapering, one needs to know that cochlear gain arises through two mechanisms: The most familiar, of course, is the pumping action (electromotility) of the outer hair cells. Less well known are purely hydrodynamic effects arising from cochlear geometry. Modelling experiments in which a fixed organ of Corti is “transplanted” into ducts of different heights demonstrate that cochlear gain is determined not only by the OHCs, but also by the hydrodynamic environment in which the hair

cells find themselves (Shera et al. 2005). Effectively, taller ducts make it easier for the outer hair cells to move the partition, and so it moves more. Thus, high-frequency sounds that peak in the base, where the duct is relatively tall, receive a major boost from the hydrodynamics; low-frequency sounds that peak in the apex, where the duct is shorter, receive less. In this way, tapering creates spatial variations in cochlear gain, and in all things that accompany it, including the sharpness of frequency tuning and the associated response delays. The tapered geometry of the cochlea—a geometry that bears an apt and striking resemblance to a miniature ear horn—bestows upon the cochlea some extraordinary acoustic properties. These properties, manifest in the remarkable sound rainbow, create significant spatial variations in cochlear responses and enhance the signal-processing capabilities of the inner ear.

Diagnosing Hearing Loss with Reflection and Distortion Otoacoustic Emissions

Carolina Abdala

The analysis by Shera and Altoè shows how OAEs provide information about fundamental cochlear mechanics. Because OAEs depend on cochlear health and are relatively non-invasive, emissions can be a powerful tool for characterizing human hearing loss. Next, Carolina Abdala describes how different kinds of OAEs can reveal complementary information about cochlear function and dysfunction.

It is now recognized that OAEs arise by one (or a combination) of two basic mechanisms within the cochlea, *nonlinear distortion* and *coherent reflection* (Shera and Guinan 1999). Past work has confirmed that distortion- and reflection-type OAEs can be impacted independently by various factors, suggesting that the two OAE classes provide non-redundant

information about cochlear function and dysfunction. Although the two emissions arise through distinct cochlear mechanisms, they share a common dependence on outer hair cell (OHC) electromotility, which provides the amplification needed to successfully detect and measure OAEs in the ear canal. Hence, both reflection and distortion emissions are linked to and provide a remote gauge of OHC electromotility.

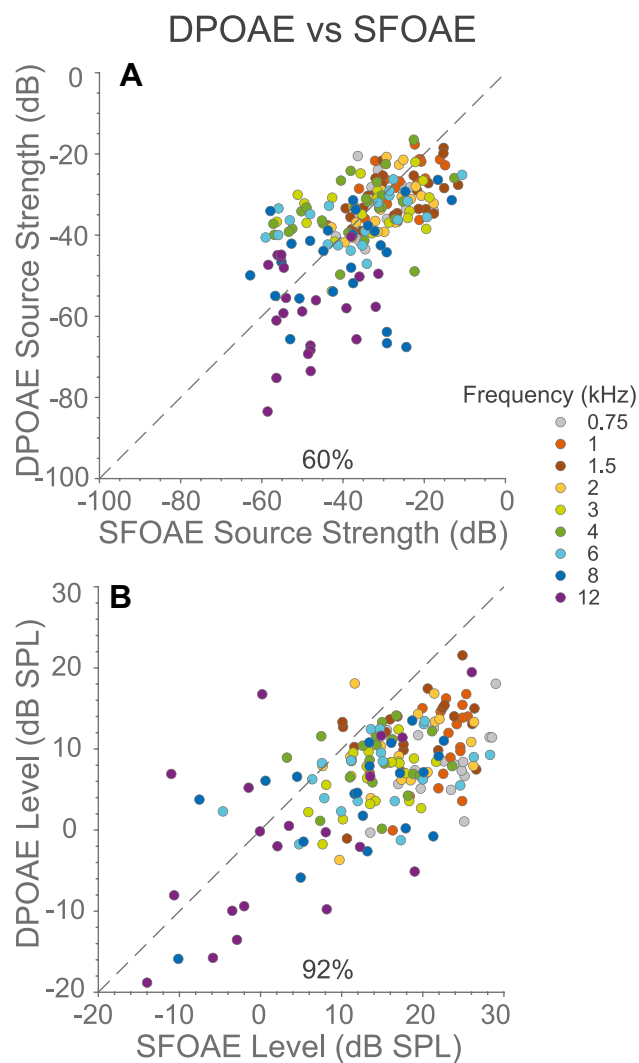


Fig. 5 A normative Joint-OAE Profile of emission source strength (A) and level (B) from 20 normal hearing adults. Each circle represents a paired SFOAE-DPOAE measurement from the same ear. Frequency is denoted by colour. The numerical value in the lower right of each panel indicates the percentage of points falling below the diagonal. In these normal-hearing ears, **A** the mechanisms generating SFOAEs are slightly stronger than those generating DPOAEs (60 % of the points fall below the diagonal) and **B** SFOAE levels are higher than those of DPOAEs measured at a fixed stimulus level, 65 dB FPL (92 % of the data fall below the diagonal). Some mild-moderate sensory hearing losses disrupt this characteristic relationship between distortion-reflection OAEs. We are currently studying these disruptions to better characterize hearing loss and enhance diagnosis

Here, we measured both classes of emissions in a group of 20 normal hearing adults and 17 mild-to-moderately hearing-impaired ears to exploit the unique generation mechanisms of each OAE in characterizing cochlear function. The $2f_1-f_2$ distortion-product OAE (DPOAE) was unmixed to isolate its distortion component, while the stimulus-frequency OAE (SFOAE) was recorded as a gauge of cochlear reflection. We presented rapid, swept-tone stimuli to evoke DPOAE and SFOAEs in an interleaved fashion over a 5-octave frequency range (0.5–16 kHz) at 10–12 stimulus levels. Novel OAE metrics characterizing the strength (OAE level re: stimulus level at the steepest point on the input/output function) and compressive properties of both OAEs were calculated using advanced fitting and analysis methods and analyzed in a *relational* manner to create a Joint-OAE Profile (Abdala and Kalluri 2017).

In normal-hearing young-adult ears, using the selected measurement parameters, we saw a characteristic relationship between the generation of nonlinear-distortion and coherent-reflection emissions: (1) SFOAEs have slightly greater source strength than DPOAEs and higher levels overall (Fig. 5A, B) and (2) SFOAE Input/Output functions show a “compression knee” at higher stimulus levels than DPOAEs (i.e., have an extended linear range) and have steeper compressive growth beyond the knee. In hearing-impaired ears, we find that OAE values fall mostly outside the normative Joint-OAE Profile distribution and can be identified as impaired with high accuracy using joint OAE strength and level measures (92–100 % hit rate). Furthermore, the distortion and reflection OAEs generated in hearing-impaired ears are not affected in a

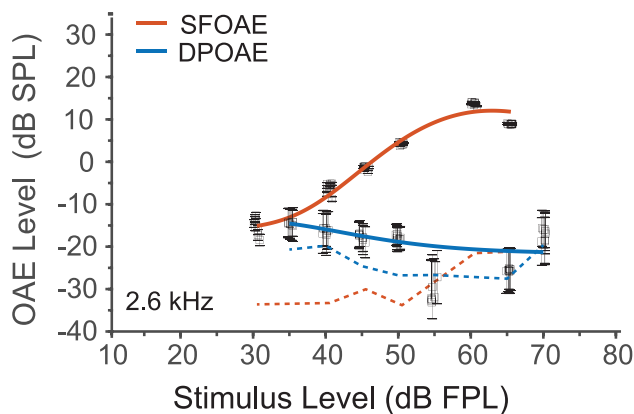


Fig. 6 SFOAE and DPOAE input/output functions at 2.6 kHz for one ear with diagnosed endolymphatic hydrops. Multiple measurements were taken at each stimulus level as displayed by the open box symbols (error bars reflect the SNR of each data point). The solid red and blue lines are a least squares fit to the OAE data, while the mean noise floors are shown as dashed lines. At this frequency, the DPOAE was not measurable above the noise floor for any stimulus level, whereas the SFOAE showed relatively typical growth and near-normal levels as the stimulus level increased. This same pattern was observed at lower frequencies as well (1 and 1.8 kHz)

uniform way. For example, one subject with endolymphatic hydrops showed strongly reduced or non-measurable nonlinear distortion OAEs but present and near-normal SFOAEs (see Fig. 6), prompting us to speculate about the pathological processes that would disrupt the generation of nonlinear distortion emissions while leaving reflection intact. Since the initial subject was tested, we have seen this same pattern in many more ears and consider it a “signature” Joint-OAE Profile for endolymphatic hydrops. We are currently exploring patterns of OAE disruption for other documented aetiologies of hearing loss as well.

In summary, our preliminary work suggests that a Joint-OAE Profile, exploiting two distinct intracochlear generation mechanisms, may better distinguish among hearing losses that have a similar audiogram but different aetiologies, underlying pathologies, and perceptual difficulties.

Efferent Control of Cochlear Amplification: an Evolutionary Perspective

Ana Belén Elgoyhen

A signature feature of cochlear organization is the separation of afferent output and efferent input, with inner hair cells sending most of the afferent cochlear input to the brain and outer hair cells receiving much of the efferent output of the brain to the cochlea. Olivocochlear efferent synapses on OHCs release acetylcholine onto specialized nicotinic receptors, modulating the hair cell membrane potential and the gain of OHC electromotility. Here, Ana Belén Elgoyhen reviews the evolution of the $\alpha 9/\alpha 10$ nicotinic receptors that are unique to hair cells and the implications for brain control of OHC electromotility and function.

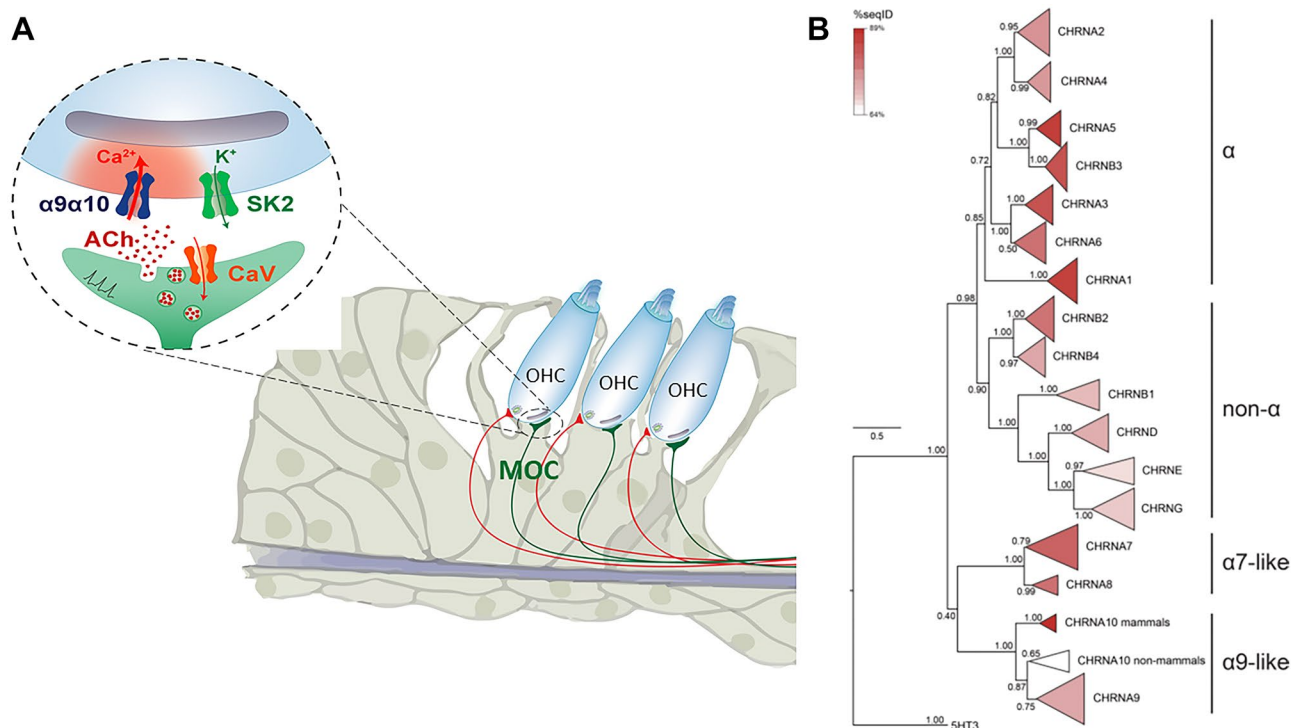


Fig. 7 **A** Schematics of the medial olivocochlear efferent-outer cell synapse. Acetylcholine released from efferent terminals binds to $\alpha 9\alpha 10$ nAChRs. In mammals, these receptors are highly calcium permeable. Intracellular calcium rise activates nearby SK2 potassium channels, leading to hair cell hyperpolarization. *Graphics by Marcelo Moglie.* **B** Phylogenetic relationships between vertebrate nicotinic subunits. The branches corresponding to the same subunits of different species were collapsed up to the node at which one subunit separates from its closest neighbour. Triangle length denotes the divergence on sequence identity from the subunit node. Triangles were coloured according to the average percentage of sequence identity between all pairs of sequences. The numbers in branches indicate

the bootstrap value obtained after 1000 replicates. Note the analysis shows that $\alpha 10$ subunits are unique in presenting a segregated grouping of orthologues with non-mammalian $\alpha 10$ subunits as a sister group to all $\alpha 9$ subunits, and mammalian $\alpha 10$ subunits an outgroup to the $\alpha 9$ /non-mammalian $\alpha 10$ branch. This reflects the overall low % sequence identity of all vertebrate $\alpha 10$ subunits, coupled to high sequence conservation within individual clades, together with the higher rate of non-synonymous substitutions reported for the mammalian clade.

Modified from Marcovich et al. 2020 under the Creative Commons license (<http://creativecommons.org/licenses/by/4.0/>)

Upon the transition to land, the hearing organs of tetrapods underwent parallel evolutionary processes, mainly due to the independent emergence of the tympanic middle ear in separate groups of amniotes (Manley 2017). This was followed by other adaptations, like the independent elongation of the auditory sensory epithelia, leading to the extension of the hearing range to higher frequencies and the parallel diversification of hair cell types with differential functions in mammals: phonoreception provided by inner hair cells and sound amplification by outer hair cells (Koppl 2011). In addition, OHCs acquired electromotility (Brownell et al. 1985), a novel mammalian amplification system based on the motor protein prestin (Dallos 2008). Efferent innervation to hair cells is an ancestral feature common to all vertebrate species (Sienknecht et al. 2014). However, only in mammals is the medial olivocochlear efferent system specialized to modulate prestin-driven OHC electromotility. Based on this observation, we have suggested that mammalian clade-specific evolutionary processes have shaped the efferent system and we have searched for adaptations on hair cell-specific proteins at the molecular level.

Medial olivocochlear efferent innervation to OHCs is cholinergic (Fig. 7A) and is mediated by $\alpha 9\alpha 10$ nicotinic acetylcholine receptors (nAChRs) present at the base of OHCs (Elgoyhen et al. 1994, 2001; Elgoyhen and Katz 2012; Gomez-Casati et al. 2005). Although the $\alpha 9$ and $\alpha 10$ subunits belong to the acetylcholine pentameric family of ligand-gated ion channels, they are distant members and have a distinct pharmacological profile (Elgoyhen et al. 1994, 2001; Rothlin et al. 1999, 2003; Verbitsky et al. 2000). The atypical features of the $\alpha 9\alpha 10$ receptor prompted the hypothesis that $\alpha 9$ and $\alpha 10$ subunits have undergone a distinct evolutionary history within the family of nAChRs. Using codon-based likelihood models (Fig. 7B), we have shown that mammalian, but not non-mammalian, $\alpha 10$ subunits have been under positive selection pressure and acquired a greater than expected number of non-synonymous amino acid substitutions in their coding region (Elgoyhen and Franchini 2011; Franchini and Elgoyhen 2006). Moreover, we have shown that mammalian-specific amino acid substitutions in the $\alpha 9$ subunit are the basis for the higher relative calcium permeability of mammalian $\alpha 9\alpha 10$ receptors (Lipovsek et al. 2014; Marcovich et al. 2020). Overall, the distinct evolutionary history of mammalian $\alpha 9\alpha 10$ nAChRs has resulted in differential calcium permeability, current–voltage relationship, channel desensitization profile, and choline efficacy across vertebrate species (Lipovsek et al. 2014, 2012; Marcovich et al. 2020). In addition, loss of functional homomeric $\alpha 10$ receptors (Elgoyhen et al. 2001; Lipovsek et al. 2012; Sgard et al. 2002) and a non-equivalent contribution of subunit interfaces to functional receptor binding sites in mammals have evolved (Boffi et al. 2017). These multiple functional adaptations of the hair cell nicotinic receptor might prove fundamental to faithfully reproduce the high

frequency activity of efferent medial olivocochlear fibres (Ballesterio et al. 2011) to fine tune the OHC cochlear amplifier, contributing to the expansion of the mammalian hearing range. It is worth noting that this evolutionary trajectory of $\alpha 9$ and $\alpha 10$ subunits is unique within the family of nAChRs, since the entire complement of nAChR subunits is highly conserved across vertebrates and even more so in tetrapods (Dent 2006), suggesting an overall gene family-wide negative selection pressure for the loss of paralogs.

The acquisition of novel functions in vertebrate auditory systems by the selection during evolution of non-synonymous substitutions at the protein level is not restricted to the efferent system. Thus, prestin, together with βV giant spectrin, a major component of the outer hair cells' cortical cytoskeleton which is necessary for electromotility, show signatures of positive selection in the mammalian clade and this may relate to the acquisition of somatic electromotility (Cortese et al. 2017; Franchini and Elgoyhen 2006). In addition, a recent high throughput evolutionary analysis identified signatures of positive selection in 167 inner-ear expressed genes in the mammalian lineage (Pisciottano et al. 2019). Therefore, the evolutionary processes of the auditory system follow the proposal that evolution is a conservative process, since existing structures tend to be modified to accomplish new tasks, rather than the de novo development of functions or structures (Manley 2000). In line with this, our work indicates that evolution-driven modifications in the $\alpha 9\alpha 10$ nAChR most likely rendered a medial olivocochlear system highly tuned to serve a differential function in the mammalian cochlea.

Funding J. S. Oghalai and J. B. Dewey: Caruso Dept. of Otolaryngology and NIH/NIDCD Grants R01 DC014450, DC013774, and DC017741 to J.S.O., and NIH/NIDCD Grants F32 DC016211 and R21 DC019209 to J.B.D. E. S. Olson, C. E. Strimbu, and Y. Wang: NIH/NIDCD Grant R01 DC015362. C. A. Shera and A. Altoè: Caruso Dept. of Otolaryngology and NIH/NIDCD Grants R01 DC003687. C. Abdala: NIH/NIDCD Grants R01 DC003552 and R01 DC003687. A. B. Elgoyhen: NIH/NIDCD Grant R01 DC001508. R. A. Eatock: NIH/NIDCD Grant R01 DC012347. R. M. Raphael: NIH/NIDCD Grant R01 DC012347.

Declarations

Conflict of Interest The authors declare no competing interests.

References

- Abdala C, Kalluri R (2017) Towards a joint reflection-distortion otoacoustic emission profile: Results in normal and impaired ears. *J Acoust Soc Am* 142:812
- Altoè A, Shera CA (2020a) The cochlear ear horn: geometric origin of tonotopic variations in auditory signal processing. *Sci Rep* 10:20528
- Altoè A, Shera CA (2020b) Nonlinear cochlear mechanics without direct vibration-amplification feedback. *Phys Rev Res* 2:013218

- Ashmore J (2008) Cochlear outer hair cell motility. *Physiological Reviews* 88(1):173–210
- Ashmore JF (1987) A fast motile response in guinea-pig outer hair cells: the cellular basis of the cochlear amplifier. *J Physiol* 388:323–347
- Ballestero J, de San Z, Martin J, Goutman J, Elgoyhen AB, Fuchs PA, Katz E (2011) Short-term synaptic plasticity regulates the level of olivocochlear inhibition to auditory hair cells. *J Neurosci* 31:14763–14774
- Bavi N, Clark MD, Contreras GF, Shen R, Reddy BG et al (2021) The conformational cycle of prestin underlies outer-hair cell electromotility. *Nature* 600(7889):553–558
- Boffi JC, Marcovich I, Gill-Thind JK, Corradi J, Collins T et al (2017) Differential contribution of subunit interfaces to $\alpha 9\alpha 10$ nicotinic acetylcholine receptor function. *Mol Pharmacol* 91:250–262
- Brownell WE, Bader CR, Bertrand D, de Ribaupierre Y (1985) Evoked mechanical responses of isolated cochlear outer hair cells. *Science* 227:194–196
- Butan C, Song Q, Bai J, Tan W, Navaratnam D, Santos-Sacchi J (2022) Single particle cryo-EM structure of the outer hair cell motor protein prestin. *Nat Commun* 13(1):290
- Carney LH, McDuffy MJ, Shekhter I (1999) Frequency glides in the impulse responses of auditory-nerve fibers. *J Acoust Soc Am* 105:2384–2391
- Cedolin L, Delgutte B (2005) Pitch of complex tones: rate-place and interspike interval representations in the auditory nerve. *J Neurophysiol* 94:347–362
- Cortese M, Papal S, Pisciotto F, Elgoyhen AB, Hardelin JP et al (2017) Spectrin betaV adaptive mutations and changes in subcellular location correlate with emergence of hair cell electromotility in mammals. *Proc Natl Acad Sci USA* 114:2054–2059
- Dallos P (2008) Cochlear amplification, outer hair cells and prestin. *Curr Opin Neurobiol* 18:370–376
- Dallos P, Zheng J, Cheatham MA (2006) Prestin and the cochlear amplifier. *J Physiol* 576(Pt1):37–42
- de Boer E (1983) On active and passive cochlear models—Toward a generalized analysis. *J Acous Soc Am* 73(2):574–576
- Dent JA (2006) Evidence for a diverse Cys-loop ligand-gated ion channel superfamily in early bilateria. *J Mol Evol* 62:523–535
- Dewey JB, Altoè A, Sera CA, Applegate BE, Oghalai JS (2021) Cochlear outer hair cell electromotility enhances organ of Corti motion on a cycle-by-cycle basis at high frequencies in vivo. *Proc Natl Acad Sci USA* 118(43):e2025206118
- Dewey JB, Applegate BE, Oghalai JS (2019) Amplification and suppression of traveling waves along the mouse organ of Corti: evidence for spatial variation in the longitudinal coupling of outer hair cell-generated forces. *J Neurosci* 39:1805–1816
- Elgoyhen AB, Franchini LF (2011) Prestin and the cholinergic receptor of hair cells: positively-selected proteins in mammals. *Hear Res* 273:100–108
- Elgoyhen AB, Johnson DS, Boulter J, Vetter DE, Heinemann S (1994) $\alpha 9$: an acetylcholine receptor with novel pharmacological properties expressed in rat cochlear hair cells. *Cell* 79:705–715
- Elgoyhen AB, Katz E (2012) The efferent medial olivocochlear-hair cell synapse. *J Physiol Paris* 106:47–56
- Elgoyhen AB, Vetter D, Katz E, Rothlin C, Heinemann S, Boulter J (2001) $\alpha 10$: a determinant of nicotinic cholinergic receptor function in mammalian vestibular and cochlear mechanosensory hair cells. *Proc Natl Acad Sci USA* 98:3501–3506
- Fallah E, Strimbu CE, Olson ES (2019) Nonlinearity and amplification in cochlear responses to single and multi-tone stimuli. *Hear Res* 377:271–281
- Fettiplace R (2020) Diverse mechanisms of sound frequency discrimination in the vertebrate cochlea. *Trends Neurosci* 43(2):88–102
- Franchini LF, Elgoyhen AB (2006) Adaptive evolution in mammalian proteins involved in cochlear outer hair cell electromotility. *Mol Phylogenet Evol* 41:622–635
- Frank G, Hemmert W, Gummer AW (1999) Limiting dynamics of high-frequency electromechanical transduction of outer hair cells. *Proc Natl Acad Sci USA* 96:4420–4425
- Gao SS, Wang R, Raphael PD, Moayed Y, Groves AK et al (2014) Vibration of the organ of Corti within the cochlear apex in mice. *J Neurophysiol* 112:1192–1204
- Ge J, Elferich J, Dehghani-Ghahnaviyeh S, Zhao Z, Meadows M et al (2021) Molecular mechanism of prestin electromotive signal amplification. *Cell* 184(4669–79):e13
- Geertsma ER, Chang YN, Shaik FR, Neldner Y, Pardon E et al (2015) Structure of a prokaryotic fumarate transporter reveals the architecture of the SLC26 family. *Nat Struct Mol Biol* 22:803–808
- Gold T (1948) Hearing. II. The physical basis of the action of the cochlea. *Proc Roy Soc London B* 135:492–498
- Gomez-Casati ME, Fuchs PA, Elgoyhen AB, Katz E (2005) Biophysical and pharmacological characterization of nicotinic cholinergic receptors in cochlear inner hair cells. *J Physiol* 566:103–118
- Housley GD, Ashmore JF (1992) Ionic currents of outer hair cells isolated from the guinea-pig cochlea. *J Physiol* 448:73–98
- Hubbard AE, Mountain DC (1983) Alternating current delivered into the scala media alters sound pressure at the eardrum. *Science* 222:510–512
- Iwasa KH (2017) Negative membrane capacitance of outer hair cells: electromechanical coupling near resonance. *Sci Rep* 7:12118
- Johnson SL, Beurg M, Marcotti W, Fettiplace R (2011) Prestin-driven cochlear amplification is not limited by the outer hair cell membrane time constant. *Neuron* 70:1143–1154
- Kemp DT (1978) Stimulated acoustic emissions from within the human auditory system. *J Acoust Soc Am* 64:1386–1391
- Khanna SM, Leonard DG (1982) Basilar membrane tuning in the cat cochlea. *Science* 215:305–306
- Kim DO, Molnar CE, Pfeiffer RR (1973) A system of nonlinear differential equations modeling basilar-membrane motion. *J Acoust Soc Am* 54:1517–1529
- Koppl C (2011) Birds - same thing, but different? Convergent evolution in the avian and mammalian auditory systems provides informative comparative models. *Hear Res* 273:65–71
- Lee HY, Raphael PD, Park J, Ellerbee AK, Applegate BE, Oghalai JS (2015) Noninvasive in vivo imaging reveals differences between tectorial membrane and basilar membrane traveling waves in the mouse cochlea. *Proc Natl Acad Sci USA* 112:3128–3133
- Lipovsek M, Fierro A, Perez EG, Boffi JC, Millar NS et al (2014) Tracking the molecular evolution of calcium permeability in a nicotinic acetylcholine receptor. *Mol Biol Evol* 31:3250–3265
- Lipovsek M, Im GJ, Franchini LF, Pisciotto F, Katz E et al (2012) Phylogenetic differences in calcium permeability of the auditory hair cell cholinergic nicotinic receptor. *Proc Natl Acad Sci USA* 109:4308–4313
- Mammano F, Ashmore JF (1996) Differential expression of outer hair cell potassium currents in the isolated cochlea of the guinea-pig. *J Physiol* 496(Pt 3):639–646
- Manley GA (2000) Cochlear mechanisms from a phylogenetic viewpoint. *Proc Natl Acad Sci USA* 97:11736–11743
- Manley GA (2017) The mammalian Cretaceous cochlear revolution. *Hear Res* 352:23–29
- Marcovich I, Moglie MJ, Carpaneto Freixas AE, Trigila AP, Franchini LF et al (2020) Distinct evolutionary trajectories of neuronal and hair cell nicotinic acetylcholine receptors. *Mol Biol Evol* 37:1070–1089
- Mistrik P, Daudet N, Morandell K, Ashmore JF (2012) Mammalian prestin is a weak Cl(-)/HCO(3)(-) electrogenic antiporter. *J Physiol* 590:5597–5610
- Neely ST, Kim DO (1983) An active cochlear model showing sharp tuning and high sensitivity. *Hear Res* 9(2):123–130
- Olson ES, Strimbu CE (2020) Cochlear mechanics: new insights from vibrometry and Optical Coherence Tomography. *Curr Opin Physiol* 18:56–62

- Pisciottano F, Cinalli AR, Stopiello JM, Castagna VC, Elgoyhen AB et al (2019) Inner ear genes underwent positive selection and adaptation in the mammalian lineage. *Mol Biol Evol* 36:1653–1670
- Puria S, Allen JB (1991) A parametric study of cochlear input impedance. *J Acoust Soc Am* 89:287–309
- Rabbitt RD (2020) The cochlear outer hair cell speed paradox. *Proc Natl Acad Sci USA* 117:21880–21888
- Rhode WS (1971) Observations of the vibration of the basilar membrane in squirrel monkeys using the Mössbauer technique. *J Acoust Soc Am* 49: Suppl 2:1218
- Rothlin C, Verbitsky M, Katz E, Elgoyhen A (1999) The $\alpha 9$ nicotinic acetylcholine receptor shares pharmacological properties with type A γ -aminobutyric acid, glycine and type 3 serotonin receptors. *Molec Pharmacol* 55:248–254
- Rothlin CV, Lioudyno MI, Silbering AF, Plazas PV, Casati ME et al (2003) Direct interaction of serotonin type 3 receptor ligands with recombinant and native $\alpha 9$ $\alpha 10$ -containing nicotinic cholinergic receptors. *Mol Pharmacol* 63:1067–1074
- Santos-Sacchi J, Iwasa KH, Tan W (2019) Outer hair cell electromotility is low-pass filtered relative to the molecular conformational changes that produce nonlinear capacitance. *J Gen Physiol* 151:1369–1385
- Santos-Sacchi J, Tan W (2018) The frequency response of outer hair cell voltage-dependent motility is limited by kinetics of prestin. *J Neurosci* 38:5495–5506
- Santos-Sacchi J, Tan W (2020) Complex nonlinear capacitance in outer hair cell macro-patches: effects of membrane tension. *Sci Rep* 10:6222
- Sasmal A, Grosh K (2019) Unified cochlear model for low- and high-frequency mammalian hearing. *Proc Natl Acad Sci USA* 116:13983–13988
- Sgard F, Charpentier E, Bertrand S, Walker N, Caput D et al (2002) A novel human nicotinic receptor subunit, $\alpha 10$, that confers functionality to the $\alpha 9$ -subunit. *Molec Pharmacol* 61:150–159
- Shera CA (2001) Frequency glides in click responses of the basilar membrane and auditory nerve: their scaling behavior and origin in traveling-wave dispersion. *J Acoust Soc Am* 109:2023–2034
- Shera CA, Guinan JJ Jr (1999) Evoked otoacoustic emissions arise by two fundamentally different mechanisms: a taxonomy for mammalian OAEs. *J Acoust Soc Am* 105:782–798
- Shera CA, Guinan JJ Jr, Oxenham AJ (2010) Otoacoustic estimation of cochlear tuning: validation in the chinchilla. *J Assoc Res Otolaryngol* 11:343–365
- Shera CA, Tubis A, Talmadge CL (2005) Coherent reflection in a two-dimensional cochlea: short-wave versus long-wave scattering in the generation of reflection-source otoacoustic emissions. *J Acoust Soc Am* 118:287–313
- Shera CA, Zweig G (1991) A symmetry suppresses the cochlear catastrophe. *J Acoust Soc Am* 89:1276–1289
- Sienknecht UJ, Köppl C, Fritzsche B (2014) Evolution and development of hair cell polarity and efferent function in the inner ear. *Brain Behav Evol* 83:150–161
- Strimbu CE, Wang Y, Olson ES (2020) Manipulation of the endocochlear potential reveals two distinct types of cochlear nonlinearity. *Biophys J* 119:2087–2101
- Tobin M, Chaiyasitdhi A, Michel V, Michalski N, Martin P (2019) Stiffness and tension gradients of the hair cell's tip-link complex in the mammalian cochlea. *Elife* 8:e43473
- Vavakou A, Cooper NP, van der Heijden M (2019) The frequency limit of outer hair cell motility measured in vivo. *Elife* 8:e47667
- Vater M, Kössl M (2011) Comparative aspects of cochlear functional organization in mammals. *Hear Res* 273(1-2):89–99
- Verbitsky M, Rothlin C, Katz E, Elgoyhen AB (2000) Mixed nicotinic-muscarinic properties of the $\alpha 9$ nicotinic cholinergic receptor. *Neuropharmacology* 39:2515–2524
- Walter JD, Sawicka M, Dutzler R (2019) Cryo-EM structures and functional characterization of murine Slc26a9 reveal mechanism of uncoupled chloride transport. *Elife* 8:e46986
- Wang Y, Fallah E, Olson ES (2019) Adaptation of cochlear amplification to low endocochlear potential. *Biophys J* 116:1769–1786
- Zheng J, Shen W, He DZ, Long KB, Madison LD, Dallos P (2000) Prestin is the motor protein of cochlear outer hair cells. *Nature* 405:149–155
- Zweig G, Shera CA (1995) The origin of periodicity in the spectrum of evoked otoacoustic emissions. *J Acoust Soc Am* 98:2018–2047

Publisher's Note Springer Nature remains neutral with regard to jurisdictional claims in published maps and institutional affiliations.

Springer Nature or its licensor (e.g. a society or other partner) holds exclusive rights to this article under a publishing agreement with the author(s) or other rightsholder(s); author self-archiving of the accepted manuscript version of this article is solely governed by the terms of such publishing agreement and applicable law.